

06.4;08.3;13.1

Manifestation of Quantum Size Effect in Polycrystalline Graphene under Ultrahigh Pressures

© D.A. Prokhorov^{1,2}, S.M. Zuev^{1,2}

¹ State Research Center of the Russian Federation Central Research Automobile and Automotive Engines Institute, Moscow, Russia

² MIREA - Russian Technological University, Moscow, Russia
E-mail: prohorovdmirii97@yandex.ru, sergei.zuev@mail.ru

Received May 28, 2024

Revised July 17, 2024

Accepted July 29, 2024

The manifestation of the quantum size effect (QSE) was investigated in polycrystalline powdered graphene produced by mechanically exfoliating graphite in water followed by drying (Gf) under various pressing pressures (up to 0.4 GPa). The QSE was characterized by a discontinuous increase in physical properties (thermal and temperature conductivity), measured using the laser flash analysis (LFA) method and differential scanning calorimetry (DSC). Non-contact surface topography measurements of Gf were performed using optical profilometry (OP).

Keywords: Quantum size effect, two-dimensional allotropic modification of carbon, polycrystalline graphene, ultra-high pressures.

DOI: 10.61011/TPL.2024.11.59677.20003

Polycrystalline graphene in powder form (Gf) produced by mechanical exfoliation of graphite in water with subsequent drying was used as the starting material in the study of the quantum size effect (QSE) in graphene. The experimental manifestation of QSE has been observed for the first time by Lutskii et al. in 1965 [1] in thin bismuth films.

In the present study, the dependence of thermophysical properties (thermal and temperature conductivity coefficient) of Gf samples on the pressing pressure is investigated, and the surfaces obtained after pressing are compared (in contrast to the original work of Xiong et al. [2], where sheets of carbon nanofiber based on polyvinyl alcohol C₂H₄O were investigated as a thermal interface material). Measurements were also carried out to establish the relation between the Gf pressing pressure and the surface roughness.

Gf samples were compressed to thickness h under ultra-high pressures (up to 0.4 GPa) by cold dry pressing with the use of a vulcanization press with an IP-1000 hydraulic drive. Graphite is transformed into diamond by static and dynamic methods [3]. Static synthesis is carried out in the region of the carbon phase diagram where diamond is thermodynamically more stable than graphite (a catalytic method is used at pressures ranging from 4 to 10 GPa and temperatures from 1000 to 2500 K). The dynamic method utilizes shock-wave compression induced by explosives at a pressure of 30 GPa and temperatures ranging from 1000 to 3000 K. The graphite–diamond transformation is not observed within the studied range of pressing pressures and temperatures (up to +150°C).

Two non-contact methods were used to measure the roughness and relief of the Gf sample surface: optical profilometry and phase-shifting interferometry (PSI). The

temperature conductivity coefficient was determined using the laser flash analysis (LFA) method. In such experiments, the growth of temperature of the sample (up to +150°C) is measured as a function of time with a Cd–Hg–Te infrared detector. Diffraction patterns were obtained by XRD.

It is known that ultra-high pressures have an effect on interatomic distances in the crystal lattice. The relation between Grüneisen parameter γ and thermal conductivity coefficient χ is set by the Leibfried–Schlömann formula [4]:

$$\chi = \frac{3}{10\pi^3} \frac{k_B^3 M a \Theta_D^3}{\hbar^3 \gamma^2 T}, \quad (1)$$

where χ is the thermal conductivity coefficient [W/(m·K)], Θ_D is the Debye temperature [K], k_B is the Boltzmann constant ($1.381 \cdot 10^{-23}$ J/K), M is the molecular weight [kg], \hbar is the Planck constant ($6.626 \cdot 10^{-34}$ J·s), a is the lattice parameter [m], and T is temperature [K].

The value of χ in homogeneous systems may also be calculated as

$$\chi(T) = \alpha(T)\rho(T)C_p(T). \quad (2)$$

Here, ρ is the sample density [kg/m³], α is the temperature conductivity coefficient [m²/s], and C_p is the specific heat capacity at constant pressure [J/(kg·K)].

The approximate sizes of crystallites in the Gf samples may be estimated from the diffraction patterns using the Scherrer equation [3]:

$$d = \frac{K\lambda}{\beta \cos \theta}, \quad (3)$$

where d is the average size of coherent scattering regions of crystallites [nm], K is the particle shape factor, λ is the

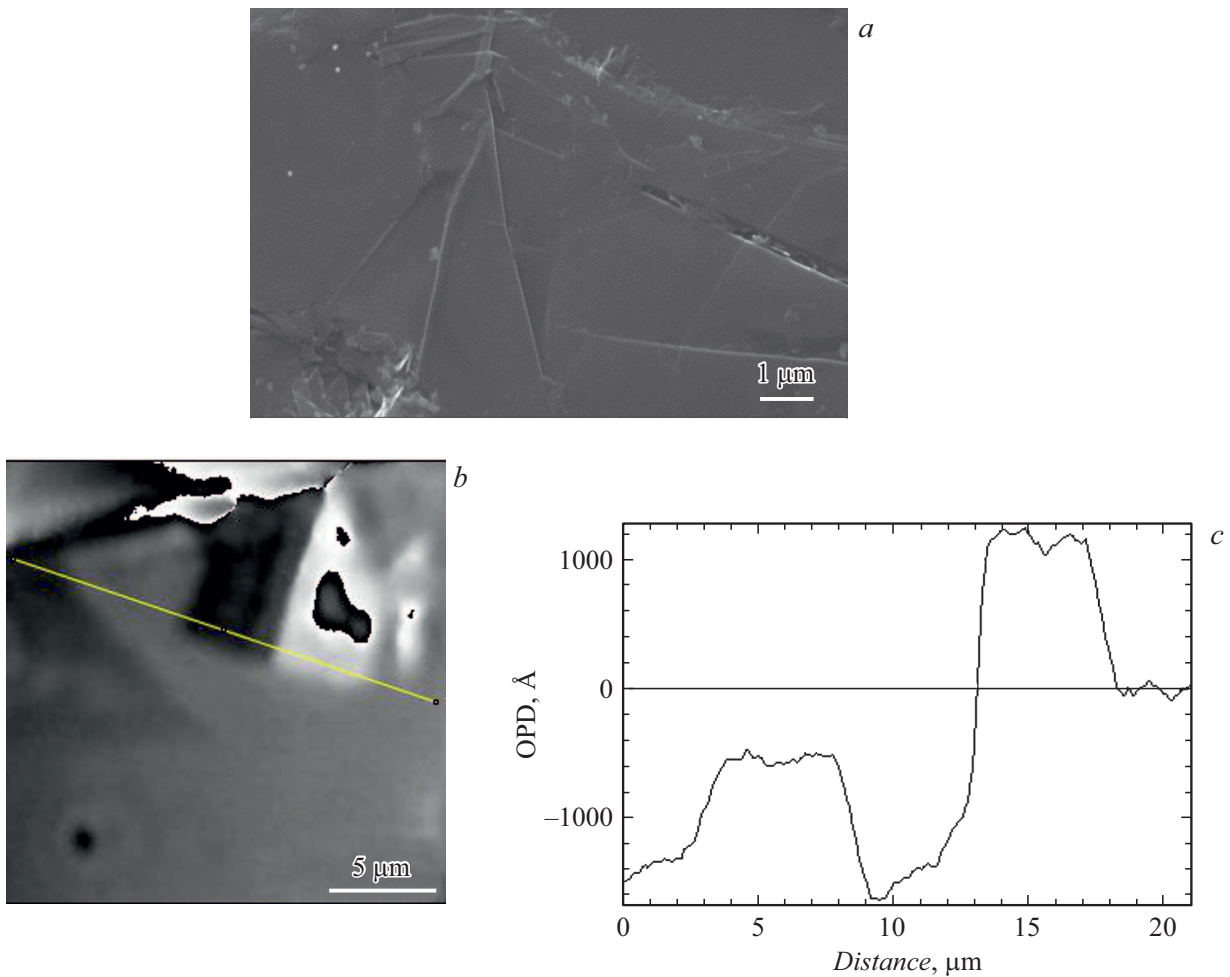


Figure 1. Images of the surface of the Gf sample pressed at a pressure of 20.0 MPa. *a* — Surface morphology; *b* — phase image with a highlighted delamination region in an unexpanded form; *c* — surface profile measured along the line shown in the left panel.

X-ray radiation wavelength [nm], β is the FWHM value of the reflection [deg], and θ is the diffraction angle [deg].

Layered regions (Fig. 1, *b*) were first identified in the scanning electron microscopy images of surfaces of the studied compressed samples (Fig. 1, *a*), and the thickness of multilayer graphene in these regions was then estimated by PSI in the process of examination of phase images (Fig. 1, *c*). The delaminated region was approximately 90 nm in height, and a similar height was determined in other areas of the sample. A Soller slit and a 0.5 mm equatorial slit were installed on the X-ray tube side, and a Soller slit, a 0.05 mm equatorial slit, and a nickel β -filter were mounted on the detector side in measurements of diffraction patterns of the examined samples.

Temperature conductivity coefficient α of the samples was measured by LFA at different temperatures. The factor of anisotropy of physical properties was not considered due to the chaotic arrangement of the initial particles and the difficulty of their subsequent orientation during pressing. Unlike the methods of a guarded hot plate, heating plates, or

thermally stimulated current, the LFA technique allows one to measure the temperature conductivity of a sample in the region of its highest values (up to 1000 mm²/s) [5]. Specific heat capacity C_p was determined by differential scanning calorimetry.

The surface roughness of the examined samples was characterized by such parameters as the arithmetic mean of absolute values of the surface deviation from the base plane (R_a), the root-mean-square value of surface heights (R_q), the average maximum profile height (an average of ten maxima and ten minima of the surface) (R_z), and the maximum height of the surface (the distance between its maximum and minimum) (R_t). Density ρ of the samples was determined after preparatory thermal conditioning at the required temperature in vacuum by direct measurements of their geometric dimensions and mass. The Gf samples were pressed by a single impact, which inevitably led to compaction of the layers, changes in crystallite sizes and Grüneisen parameter γ , and, consequently, a change in χ (see (1)). The measurements of α were performed after thermal conditioning of the samples for 60 min at a

Table 1. Results of calculations based on diffraction patterns of the studied Gf samples

p , MPa	K	λ , nm	2θ , deg	β , deg	d , nm
0.1	0.94	1.5406	$26.43 \pm \Delta_\theta$	0.3014	28.27
200.0	0.94	1.5406	$26.54 \pm \Delta_\theta$	0.1574	54.16

Note. Δ_θ is the absolute error of measurement of the diffraction angle (0.01%) [6].

constant temperature of +25, +100, and +150°C. Thermal conductivity coefficient χ was calculated by formula (2).

The PSI method allows one both to estimate the number of layers of Gf (as shown in Fig. 1) and to validate its polycrystalline structure. It was also determined in experiments that the samples are transparent in the near IR region, which is indicative of a high thermal conductivity of this material. Table 1 lists the results of calculations based on diffraction patterns of the Gf samples. The samples feature peaks around 26.55 and 54.69°, which correspond to graphite phases with orientations (002) [7] and (004). The peaks in regions from 23 to 25° and from 42 to 45° may correspond both to the graphite phase and to the graphene phase. The results of earlier studies of graphene diffraction patterns [8–10] suggest that the diffraction pattern of Gf samples corresponds to the one of graphite, but it cannot be said with certainty that it does not contain graphene. At the stage of applying pressure p , particles are packed, their contacts with each other intensify, air is removed, and the particles are shifted actively in the direction of force application (and, to a lesser extent, in the transverse direction). Pores are filled, and the particles occupy a stable position. Since the

overall contact surface area increases, the particles acquire mechanical adhesion. As p increases further, the density grows due to elastic deformation of particles in the contact region. At this point in the process of pressing, the sample retains the original size of crystallites. When $p = 200$ MPa is reached, brittle fracture (plastic flow) is initiated: the load exceeds the compressive resistance of crystallites, and they get deformed. As a result, the crystallites are redistributed and, as can be seen from Table 1, grow in size (almost by a factor of 2). Hot pressing is even more conducive to crystallite growth and, consequently, an increase in χ . The obtained dependences of χ and α on pressing pressure p are unusual for graphite. The oscillations of χ and α , which reach their maximum at p close to 44 MPa, are not unlike the oscillations of other physical properties in thin bismuth films (with a thickness ranging from 20 to 160 nm). All the measured thermophysical properties of Gf samples are presented in Table 2. The results of measurements at $p = 400$ MPa, which reveal an increase in α and χ with a reduction in temperature, suggest that a similar enhancement of amplitude of the physical properties should occur in Gf at cryogenic temperatures. The two-dimensional images of relief of the Gf samples subjected to different pressing pressures (see Fig. 2) reveal no dependence of the surface roughness on the pressing pressure. The initial average powder particle size and the roughness of the inner surface of the used press mold are the factors that govern the sample surface roughness in this case. The use of QSE in Gf allows one to raise the thermal and temperature conductivity by several orders of magnitude, which makes it relevant to the issues of cooling the electronic components of modern devices. Factors limiting the application of Gf include the difficulty of fabrication of structures with

Table 2. Results of measurement of the physical properties of the studied Gf samples

p , MPa	ρ , kg/m ³	α , 10 ⁻⁶ m ² /s	χ , W/(m·K)	h , mm	T , °C	C_p , J/(kg·K)
0.1	475	$0.35 \pm \delta_\alpha$	$0.1 \pm \delta_\chi$	2.70	+100	$602 \pm \delta_C$
1.0	475	$0.34 \pm \delta_\alpha$	$0.1 \pm \delta_\chi$	3.11		$619 \pm \delta_C$
2.3	1590	$0.79 \pm \delta_\alpha$	$1.0 \pm \delta_\chi$	2.11		$796 \pm \delta_C$
20.0	2213	$7.38 \pm \delta_\alpha$	$16.3 \pm \delta_\chi$	1.11		$998 \pm \delta_C$
44.1	1690	$42.23 \pm \delta_\alpha$	$58.7 \pm \delta_\chi$	1.90		$823 \pm \delta_C$
	1851	$42.61 \pm \delta_\alpha$	$59.0 \pm \delta_\chi$	2.25		$748 \pm \delta_C$
200.0	1810	$6.27 \pm \delta_\alpha$	$10.3 \pm \delta_\chi$	1.79		$908 \pm \delta_C$
300.0	1729	$5.85 \pm \delta_\alpha$	$11.6 \pm \delta_\chi$	0.48	$1147 \pm \delta_C$	
400.0	2587	$4.34 \pm \delta_\alpha$	$14.0 \pm \delta_\chi$	0.26	+25	$1247 \pm \delta_C$
		$3.06 \pm \delta_\alpha$	$12.0 \pm \delta_\chi$		+100	$1516 \pm \delta_C$
		$2.47 \pm \delta_\alpha$	$10.5 \pm \delta_\chi$		+150	$1643 \pm \delta_C$

Note. δ_α is the relative error of α measurement (3%) [11], δ_C is the relative error of C_p measurement (1%) [12], and δ_χ is the relative error of χ measurement (4%) [11,12] calculated based on the total error according to formula (2) with the error of ρ measurement assumed to be negligible.

a complex shape, which require special press molds, and the fact that Gf is a fine conductor of electric current.

Acknowledgments

Equipment provided by the common use center of RTU MIREA was used in this study.

Funding

This study was supported by the Russian Science Foundation, grant № 23-29-00079 (<https://rscf.ru/project/23-29-00079>).

Conflict of interest

The authors declare that they have no conflict of interest.

References

- [1] V.N. Luts'kii, V.B. Sandomirskii, Yu.F. Ogrin, I.M. Lifshits, A.M. Kosevich, *Yavlenie ostsillyatsii termodinamicheskikh i kineticheskikh svoistv plenok tverdykh tel*, State Register of Scientific Discoveries in the USSR, No. 182, priority date: May 21, 1953 (theoretical justification) and December 10, 1965 (experimental verification) (in Russian).
- [2] J. Xiong, S. Chen, Y. Choi, K. Matsugi, *Sci. Rep.*, **11**, 17183 (2021). DOI: 10.1038/s41598-021-96691-z
- [3] V.V. Prut, *Chislennyi raschet perekhoda grafita v almaz v metallicheskom Z-pinche* (Kurchatovskii Inst., M., 2007), p. 1 (in Russian).
- [4] Sh.M. Ismailov, S.M. Orakova, Z.A. Isaev, Kh.Sh. Yakh'yaeva, *High Temp.*, **59** (1), 46 (2021). DOI: 10.1134/S0018151X21010053.
- [5] I.M. Abdulagatov, B.A. Grigor'ev, Z.Z. Abdulagatova, S.N. Kallaev, A.G. Bakmaev, Z.M. Omarov, *Vesti Gazov. Nauki*, No. 1 (46), 129 (2021) (in Russian).
- [6] *Difraktometri: rentgenovskie modeli DRON-8N i DRON-8T*, Pattern Approval Certificate of Measuring Instruments No. 82575-21 (Vseross. Nauchno-Issled. Inst. Metrol., 2023) (in Russian).
- [7] J. Fayos, *J. Solid State Chem.*, **148** (2), 278 (1999). DOI: 10.1006/JSSC.1999.8448
- [8] R. Siburian, H. Sihotang, S. Lumban Raja, M. Supeno, C. Simanjuntak, *Orient. J. Chem.*, **34** (1), 182 (2018). DOI: 10.13005/ojc/340120
- [9] T.F. Emiru, D.W. Ayele, *Egypt. J. Basic Appl. Sci.*, **4** (1), 74 (2017). DOI: 10.1016/j.ejbas.2016.11.002
- [10] A. Ahmad, S. Ullah, A. Khan, W. Ahmad, A.U. Khan, U.A. Khan, A.U. Rahman, Q. Yuan, *Appl. Nanosci.*, **10** (4), 1243 (2020). DOI: 10.1007/s13204-019-01204-0
- [11] *Light-Flash-Apparatur LFA 467 HyperFlash-Serie: Methode, Technik, Applikationen zu Temperatur- und Wärmeleitfähigkeit*, Netzsch, 0823. https://analyzing-testing.netzsch.com/_Resources/Persistent/6/f/4/1/6f41f20a04ff124384a8963ed7bf4184c25e1c40/LFA_467_HyperFlash.de.web.pdf
- [12] *DSC 204 F1 Phoenix, Technical Specifications*, Netzsch, 0222. https://analyzing-testing.netzsch.com/_Resources/Persistent/b/8/6/c/b86c2a6637064b1361d580c2bc05367072b194d6/Key_Technical_Data_en_DSC_204_F1_Phoenix.pdf

Translated by D.Safin

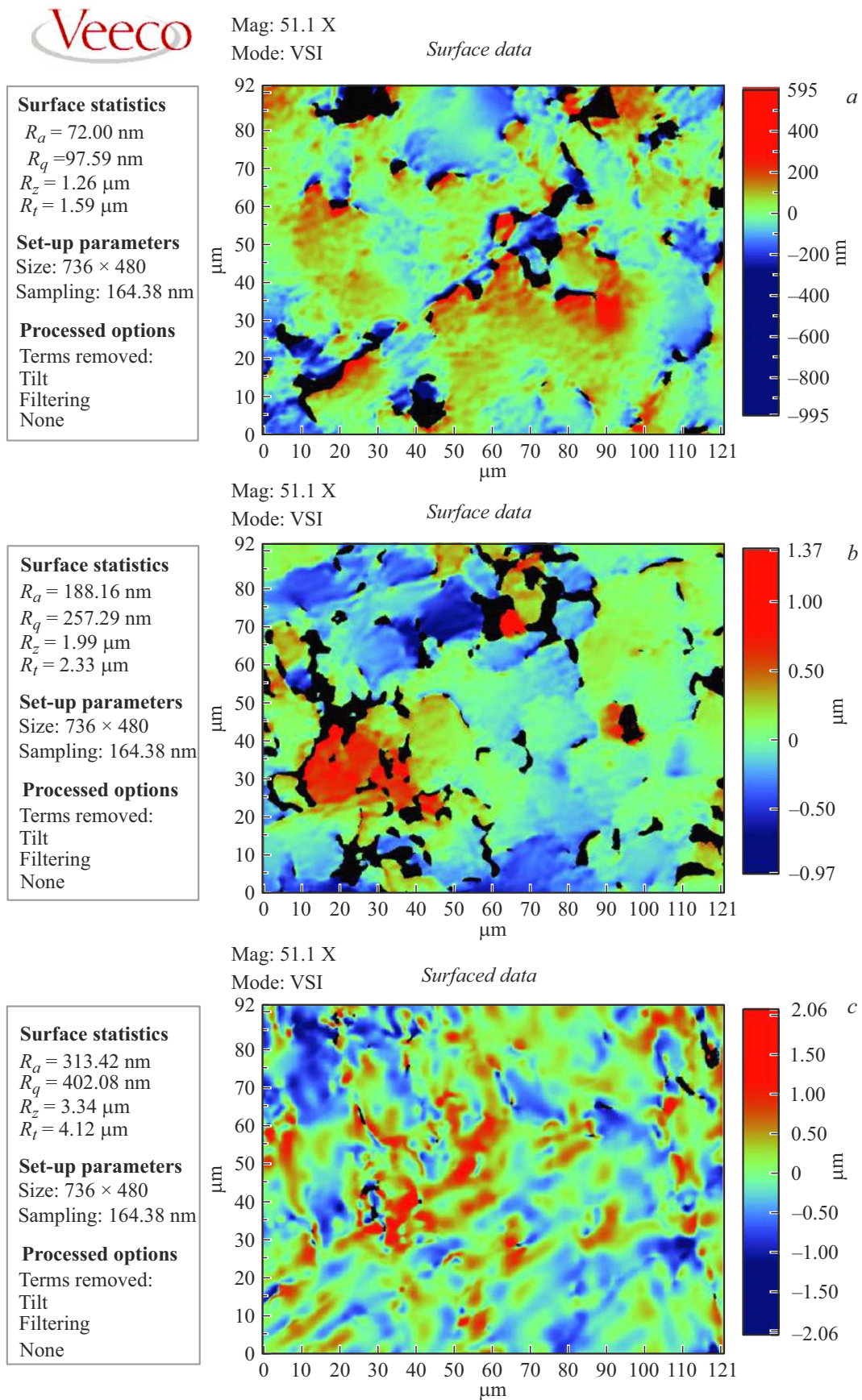


Figure 2. Surface roughness of the Gf samples pressed at $p = 20.0$ (a), 44.1 (b), and 400.0 MPa (c). $51.1\times$ magnification.